

Porous Coordination Polymer Based on Bipyridinium Carboxylate Linkers with High and Reversible Ammonia Uptake

Maxime Leroux,[†] Nicolas Mercier,^{*,†} Magali Allain,[†] Marie-Claire Dul,[†] Jens Dittmer,[‡] Abdel Hadi Kassiba,[‡] Jean-Pierre Bellat,[§] Guy Weber,[§] and Igor Bezverkhyy^{*,§}

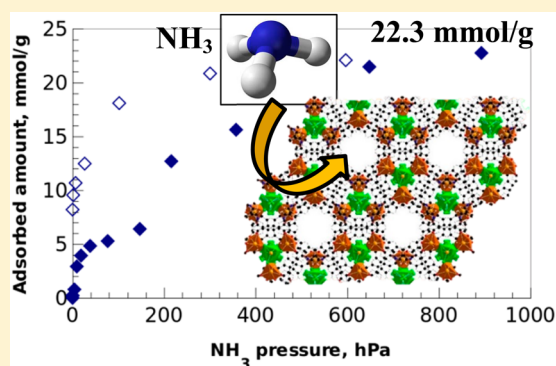
[†]MOLTECH Anjou, UMR-CNRS 6200, Université d'Angers, 2 Bd Lavoisier, 49045 Angers, France

[‡]IMMM, UMR-CNRS 6283, Université du Maine, Avenue O. Messiaen, 72085 Le Mans, France

[§]ICB, UMR-CNRS 6303, Université de Bourgogne-Franche Comté, 9 A. Savary, 21078 Dijon, France

Supporting Information

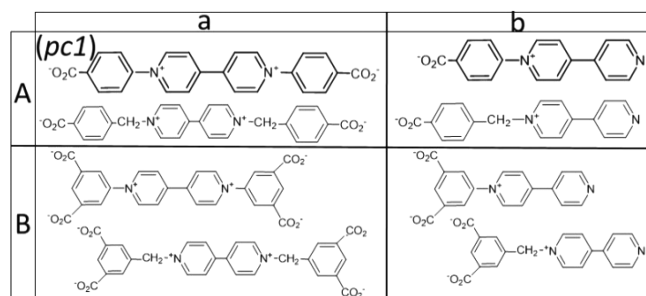
ABSTRACT: The zwitterionic bipyridinium carboxylate ligand 1,1'-bis(4-carboxyphenyl)-4,4'-bipyridinium (pc1) in the presence of cadmium chloride affords novel porous coordination polymers (PCPs): $[\text{Cd}_4(\text{pc}1)_3\text{Cl}_6] \cdot \text{CdCl}_4 \cdot \text{guest}$ (**1**) crystallizing in the $P\bar{3}1c$ space group. In the structure, $[\text{Cd}_4\text{Cl}_6(\text{CO}_2)_6]$ building units are linked together by six pc1 ligands, leading to a 3D high-symmetrical network exhibiting hexagonal channels along the c axis. The walls of this PCP consist of cationic electron-acceptor bipyridinium units. The PCP **1** reversibly adsorbs H_2O and CH_3OH up to about 0.1 g/g at saturation showing the adsorption isotherms characteristic of a moderately hydrophilic sorbent. Adsorption of ammonia (NH_3) follows a different pattern, reaching an exceptional uptake of 0.39 g/g (22.3 mmol/g) after the first adsorption cycle. Although the crystalline structure of **1** collapses after the first adsorption, the solid can be regenerated and maintains the capacity of 0.29 g/g (17 mmol/g) in the following cycles. We found that the high NH_3 uptake is due to a combination of pore filling taking place below 150 hPa and chemisorption occurring at higher pressures. The latter process was shown to involve two phenomena: (i) coordination of NH_3 molecules to Cd^{2+} cations as follows from ^{113}Cd NMR and (ii) strong donor–acceptor interactions between NH_3 molecules and pc1 ligands.



1. INTRODUCTION

Porous coordination polymers (PCPs) or metal–organic frameworks (MOFs), based on redox-active linkers of the bipyridinium type (also called *viologens*), have emerged as an interesting class of porous compounds.^{1–8} Such linkers usually consist of functional units bearing carboxylate groups anchored to the bipyridine core at the N positions, leading to zwitterionic or anionic bipyridinium carboxylate ligands (Scheme 1). These

Scheme 1. Structural Formulas of Some Zwitterionic (A), Anionic (B), Symmetrical (a), or Asymmetrical (b) Bipyridinium Carboxylate Type Ligands



kinds of ligands often lead to coordination polymer materials with dense networks as a result of the ability of linkers at the N^+ site to interact with carboxylate groups through $\text{CO}_2^- \cdots \text{N}^+$ electrostatic interactions.^{9–14} However, an interesting feature of these materials, as encountered more generally in those based on bipyridinium units,^{15–18} are their photo- or thermochromic properties due to an electron-transfer process from the carboxylate electron donor toward the bipyridinium electron acceptor, giving radical species. The color change in such an activated redox process is due to the different absorption domains of *viologen* V^{2+} or V^+ (UV) and $\text{V}^{\bullet+}$ or V^\bullet (visible).¹⁹ In such a system, a color change can also originate from the formation of charge-transfer (CT) complexes of the donor and bipyridinium acceptor (CT band in the visible region). Thus, the use of such ligands to build porous compounds appears to be very interesting not only because the redox *viologen* site is able to strongly interact with electron-rich guests but also because the donor (guest)–acceptor (host) interactions can be accompanied by a color change, which is useful for chemical sensor applications. Although PCPs based on such ligands are

Received: May 7, 2016

not easy to stabilize, some of them have been reported quite recently. Most of those with rigid 2D or 3D networks and clearly defined channels are based on bipyridinium cores consisting of one pyridinium cycle and one pyridyl chelating cycle (Scheme 1, column b).^{1–6} In contrast, those based on diquaternized bipyridinium, while better electron-acceptor units, are more scarce.^{7,8} In one example, a 3D supramolecular network results from weakly interacting 1D coordination polymers.⁷ In another example, a 3D coordination polymer that is obtained using the 1,1'-bis(4-carboxyphenyl)-4,4'-bipyridinium (pc1) ligand displays cavities difficult to access.⁸

Ammonia (NH₃) is an important compound widely used in different industrial processes but also a very toxic gas even at low concentration. The search for materials for its detection, on the one hand, or for its capture from air and safe storage and transportation, on the other hand, is an important subject from industrial and environmental points of view. PCPs have been considered as potential materials for such purposes.^{3,20–28} In particular, a bipyridinium-linker-based PCP has been proposed as a visual colorimetric sensor for NH₃ detection via a redox reaction between the NH₃ and *viologen* units, resulting in a radical-containing colored material.³ However, the detection limit has not been investigated.³ Adsorption and storage of NH₃ remain great challenges. If some materials, such as zeolites or activated carbons, are known to exhibit good adsorption capacities, the progressive desorption of NH₃ over time remains a challenging issue.^{29,30} To overcome this problem, porous structures possessing active sites able to retain NH₃ molecules are of high interest. Two main strategies have been followed in the field of PCPs: the functionalization of ligands by free Brønsted acid groups such as CO₂H or NH₃⁺^{21,22} or the introduction of Lewis acid sites.^{23–26} In most cases, the Lewis acid sites are metal ions at nodes of networks, especially Cu²⁺ as in MOF-74²³ or HKUST-1,^{25,26} which become metal open sites upon removal of initially coordinated solvent molecules. A main disadvantage of such materials is their tendency to collapse upon adsorption of NH₃ as a result of metal–NH₃ coordination and consequently a lack of reversibility and recyclability.^{25–28} In the neighboring field of covalent organic frameworks, the introduction of Brønsted acid groups³¹ or a high density of Lewis acidic boron atoms into a framework material has also been successful for NH₃ storage with an uptake of 15 mmol/g.³² Finally, PCPs with bipyridinium linkers represent another category of materials possessing Lewis acid sites.

In this context, we report on an unprecedented PCP based on the pc1 bipyridinium carboxylate linker, [Cd₄(pc1)₃Cl₆]·CdCl₄-guest (**1**), which exhibits a reversible high NH₃ uptake. The trigonal crystal structure of **1** containing channels running along the *c* axis of the hexagonal unit cell will first be described. Then, the adsorption of methanol (CH₃OH) and water (H₂O) by **1** will be described, showing the presence of open pores with moderately hydrophilic walls. Finally, the adsorption properties of **1** for NH₃ will be fully analyzed, showing that in a low-pressure range a reversible physisorption occurs, while chemisorption is observed at higher pressure. This process results in a loss of sample crystallinity; however, a high NH₃ capacity is preserved.

2. EXPERIMENTAL SECTION

2.1. Synthesis and Characterization. Materials and General Methods. All starting materials were of analytical grade and obtained from commercial sources without further purification. A 4,4'-bis(carboxyphenyl)bipyridinium dichloride dihydrate (H₂pc1Cl₂·

2H₂O) ligand was synthesized according to the literature (see the Supporting Information).³³ Thermogravimetric analyses (TGA) were performed using a TGA-2050 analyzer (TA Instruments) from room temperature to 1000 °C with a heating rate of 10 °C/min under a nitrogen flow. Powder X-ray diffraction (PXRD) analyses were measured at room temperature on a D8 Bruker diffractometer (Cu Kα, λ = 1.5418 Å) equipped with a linear Vantec superspeed detector and have shown that all of the observed reflections could be indexed in the unit cell parameters obtained from single-crystal X-ray diffraction experiments (Figure S1).

Preparation of the Compound. A mixture of H₂(pc1)Cl₂·2H₂O (50.5 mg, 0.1 mmol), cadmium chloride (CdCl₂; 128.4 mg, 0.7 mmol), dimethylformamide (1.5 mL), dioxane (1.5 mL), and H₂O (0.3 mL) was heated at 100 °C for 48 h in a 25 mL Teflon-lined stainless steel autoclave. Then the mixture was slowly cooled to room temperature at a rate of 2 °C/h. Crystals suitable for X-ray analyses were collected, washed with ethyl acetate, and air-dried: [Cd₄(pc1)₃Cl₆]·CdCl₄·8H₂O (**1**) of 60% yield based on H₂(pc1)Cl₂·2H₂O. Anal. Calcd for Cd₅Cl₁₀C₇₂H₆₄N₆O₂₀ (2249.79): C, 38.43; H, 2.86; N, 3.73. Found: C, 37.90; H, 2.62; N, 3.95.

2.2. X-ray Crystallography. X-ray diffraction data were collected on an Agilent Supernova with Cu Kα radiation (λ = 1.5418 Å). Data were collected at 180 K from a selected single crystal of **1** under a nitrogen atmosphere. A summary of crystallographic data and refinement results for **1** is listed in Table 1. The structure was solved

Table 1. Crystallographic Data for **1**

fw (g/mol)	2249.79
space group	P3̄1c
<i>a</i> , Å	18.196(5)
<i>b</i> , Å	18.196(5)
<i>c</i> , Å	15.127(5)
α, deg	90
β, deg	90
γ, deg	120
<i>V</i> , Å ³	4337(2)
<i>Z</i>	2
obsd reflns [<i>I</i> > 2σ(<i>I</i>)] (<i>R</i> _{int})	2626 (0.029)
no. of param	175
<i>R</i> ₁ [<i>I</i> > 2σ(<i>I</i>)]/ <i>wR</i> ₂ (all data)	0.0441/0.1148

by direct methods and refined on *F*² by a full-matrix least-squares method with anisotropic approximation for all non-hydrogen atoms, using the SHELXL97 package. Three H₂O molecules were located in the channels, while five others were deduced from analysis of the SQUEEZE routine of PLATON, leading to a total of eight H₂O molecules per formula unit, in good accordance with the TGA experiment. All non-hydrogen H₂O atoms were treated with a riding model. Absorption was corrected by the program SADABS. A complete list of crystallographic data, along with the atomic coordinates, anisotropic displacement parameters, and bond distances and angles for each compound, is given as a CIF file (CCDC 1473082).

2.3. Electron Paramagnetic Resonance (EPR) and NMR Measurements. Solid-state NMR experiments have been performed on a Bruker Avance III 300 MHz WB spectrometer equipped with a 2.5 mm H/X probehead. The magic-angle-spinning (MAS) frequency was 10 kHz. There is only a little heating by MAS friction at this frequency. ¹H–¹¹³Cd cross-polarization (CP) NMR spectra have been accumulated over 24 K (crystalline sample) and 29 K (after NH₃ adsorption) repetitions with contact times of 4 and 7 ms, respectively. For the sample after desorption, the only successful acquisition strategy for ¹¹³Cd was direct excitation with fast recycling (0.5 s) to 64 K repetitions. The DEPTH pulse sequence was applied for background suppression. The spectra have been referenced to an aqueous solution of Cd(ClO₄)₂.

EPR experiments were carried out at room temperature on a Bruker EMX spectrometer working at X band (9.51 GHz). Instrumental

parameters were fixed to 100 kHz and 0.5 G respectively for the frequency and magnetic field modulation, while 2 mW was used for the microwave power. These parameters allow recording of the EPR signals with good resolution and prevention of any distortion that may occur from saturation phenomena induced by a high-spin concentration. Dry 2,2-diphenyl-1-picrylhydrazyl radicals were used to evaluate the g factors in the investigated samples.

2.4. Adsorption Measurements. Adsorption–desorption isotherms of CH_3OH , H_2O , and NH_3 on **1** were measured at 298 K using a home-built McBain-type thermobalance. Before measurements the samples (ca. 15 mg) were outgassed at 423 K under vacuum (10^{-6} hPa) overnight. The detailed description of the experimental procedure can be found elsewhere.⁶ The estimated experimental error on the adsorbed amount was about 1 mg/g. The accuracy of the pressure measurement was 1%, and the temperature was maintained within 1 K. The adsorption isotherm of carbon dioxide (CO_2) in the range of 0.2–50 bar at 298 K was measured using a Rubotherm magnetic suspension balance.

3. RESULTS AND DISCUSSION

3.1. Crystal Structure Description. The asymmetric unit of the structure of **1** contains three Cd^{2+} cations, one pc1 molecule, three chlorides, and one oxygen atom assigned to a H_2O molecule. The Cd(1) atom, located at the crossing of 3-fold and 2-fold axes (3.2 special position), and the Cd(2) atom, located on a 2-fold axis, define a tetrameric building unit, as shown in Figure 1. While Cd(1) is surrounded by six chloride

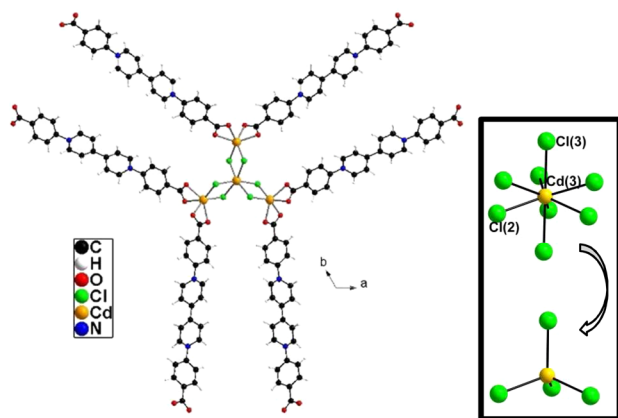


Figure 1. View of the tetrameric inorganic building unit bearing six pc1 molecules in the trigonal structure of **1** and a disordered CdCl_4^{2-} tetrahedral anion (inset).

anions in a pseudooctahedral geometry [$d = 2.641(1)$ Å],^{34,35} Cd(2) is bound to two chlorides through edge-sharing with $\text{Cd}(1)\text{Cl}_6$ octahedra and four oxygen atoms of carboxylate groups belonging to two pc1 ligands. This results in $[\text{Cd}_4\text{Cl}_6(\text{CO}_2)_6]$ building units that are linked together by six pc1 ligands to construct the porous 3D network. The positive charge of the $[\text{Cd}_4\text{Cl}_6(\text{pc}1)_3]^{2+}$ framework is balanced by the presence of isolated CdCl_4^{2-} anions located between two consecutive tetrameric cores along the c axis. Let us note that this dianion is disordered over two positions with $d[\text{Cd}(3)-\text{Cl}] = 2.447(4)$ Å (Cl2) and 2.427(9) Å (Cl3) (Figure 1, inset).

Figure 2 shows a general view of the structure of **1** along the c axis where the channels with hexagonal windows are clearly defined. The solvent molecules present in the pores have not all been located. Only one oxygen atom, assigned to a H_2O molecule, has been refined in a general position with half-occupation rate (Figure 2). The 12 symmetry-related oxygen atoms line the walls of the channels, indicating the existence of

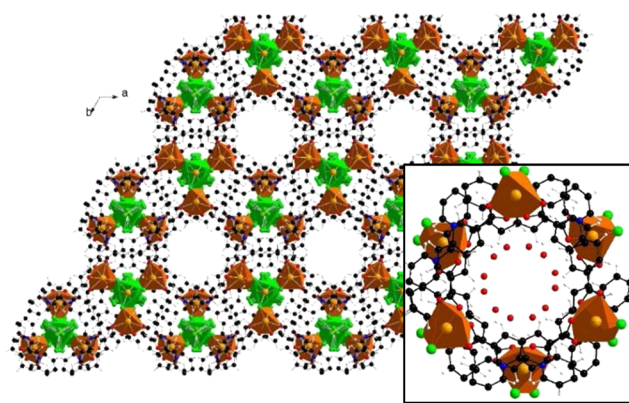


Figure 2. General view of the structure of **1** showing the hexagonal channels running along the c axis (the H_2O molecules in the pores have been omitted for clarity). Inset: View of one hexagonal channel incorporating H_2O molecules that interact with the walls of the framework through hydrogen bonding.

weak hydrogen bonds between H_2O oxygen atoms and slightly acidic hydrogen atoms of the phenyl rings of pc1 ligands borne by the carbon atoms in the β positions of N^+ sites (Figure 3).

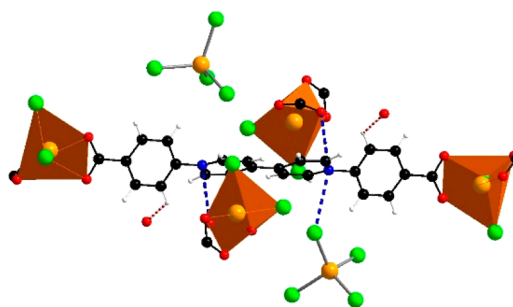


Figure 3. Details of the structure of **1** showing the environment of a bipyridinium carboxylate (pc1) ligand with neighboring CdCl_4^{2-} anions, $\text{N}^+\cdots\text{Cl}$ [$d = 3.408(8)$ Å] or $\text{N}^+\cdots\text{O}(\text{CO}_2^-)$ [$d = 3.579(8)$ Å] contacts, as well as $(\text{C})\text{H}\cdots\text{O}(\text{H}_2\text{O})$ hydrogen bonds [$d = 2.65(1)$ Å] between pc1 and the guest H_2O molecules present in the pores.

The other solvent molecules in the center of the channels may be disordered, which did not allow us their location. After removal of all of the solvent molecules, the potential of the void space has been estimated to 10% of the unit volume by the SQUEEZE routine of PLATON. Using the distance across the pore between the hydrogen atoms of the bipyridinium units (7.5 Å) and the value of van der Waals radius of hydrogen (1.2 Å), the accessible pore diameter was calculated to be close to 5 Å.

Of great interest in the field of viologen-based solid-state materials is analysis of the intermolecular interactions between the electron-acceptor bipyridinium unit and electron-donor groups in order to tentatively explain some optical properties such as colored samples due to CT bands or photo- or thermochromism. In the particular case of PCPs, the accessibility of pyridinium cycles by guest solvent molecules is especially interesting because desolvation can further afford pyridinium open sites, which would react very rapidly with electron-donor guest molecules (chemical sensor application). Unfortunately, in **1**, as in most of bipyridinium-based structures, the viologen core does quite have strong intra-framework interactions, on the one hand with a chloride

belonging to a CdCl_4^{2-} anion [$d = 3.408(8) \text{ \AA}$], and on the other hand with an oxygen atom of a carboxylate group also bonded to Cd(2) [$d = 3.579(8) \text{ \AA}$] (Figure 3). However, the high concentration of the bipyridinium units in the structure of **1** must be noted. This is a consequence of the presence of the small sized anions of Cl^- in **1**, while bulky carboxylate-type organic ligands counterbalance the positive charge of the metal cations in other such materials. Thus, a high concentration of the dipolar moments (N^+Cl^- or $\text{N}^+\cdots\text{O}^-$ types) are present in the framework and can interact through electrostatic interactions with polar guest molecules such as H_2O , HCOH , or NH_3 . These interactions probably come in addition to hydrogen bonding involving some hydrogen atoms of the p Cl molecules (Figure 3), explaining, for instance, the presence of H_2O molecules lining the walls of the channels (Figure 2).

3.2. Adsorption of CH_3OH and H_2O . The pores of **1** are not accessible for N_2 at 77 K. This could be either due to the so-called “gate effect”^{36–39} taking place in flexible structures or due to kinetic limitations for the diffusion of nitrogen molecules in small pores at cryogenic temperature.^{40,41} Given the nonflexible nature of **1** (see below), we consider that the second effect is in action. In contrast, the solid readily adsorbs CH_3OH , H_2O , and CO_2 at 298 K (Figure 4). The fully reversible character of the adsorption–desorption process for all molecules suggests that only physisorption occurs in **1** under these conditions. Such behavior is different from that of CH_3OH chemisorption observed for other bipyridinium-based phases described in our previous work.⁶ While the density of adsorbed CO_2 at 298 K is poorly defined,⁴² the density of

adsorbed H_2O and CH_3OH phases can be assumed to be equal to the density of the bulk liquid at saturation, and their isotherms can thus be used to estimate the accessible pore volume of **1**. The value determined from the maximum amount of H_2O and CH_3OH adsorbed (around 0.1 g/g) is close to 0.10 or 0.13 cm^3/g , respectively. Slightly higher pore volume probed by CH_3OH despite the smaller size of the H_2O molecule (2.64 vs 3.64 \AA) can be attributed to a higher affinity of the material toward CH_3OH (see below).

The shape of the adsorption isotherms of H_2O , CH_3OH , and CO_2 is different from that of the type I isotherms, showing a sharp knee at very low pressure.⁴³ In contrast, **1** exhibits S-shaped isotherms with negligible adsorption in the low-pressure range (clearly seen on a logarithmic relative pressure scale; Figure 4). Such behavior in PCPs can be due to either a gate-opening phenomenon or a moderate strength of the interaction between the molecules and pore walls.

The first explanation implies that during degassing the framework structure contracts, provoking shrinking of the pores, which become thus inaccessible to the adsorbate molecules. At a certain threshold pressure, the pores open enough to allow access of the molecules, giving rise to adsorption. To check this hypothesis, we recorded the PXRD pattern of the degassed sample **1** sealed in a capillary. A full profile fitting of the pattern was done using the Le Bail method⁴⁴ (Figure S2). It appears that the pattern can be successfully fitted in the initial $P31c$ space group, and the cell parameters of the degassed sample ($a = b = 18.175 \text{ \AA}$ and $c = 15.012 \text{ \AA} - RT$) are close to those of the initial sample measured in air ($a = b = 18.196 \text{ \AA}$ and $c = 15.127 \text{ \AA} - 180 \text{ K}$). This similarity allows one to rule out any pore shrinking at 298 K in degassed **1** and therefore to conclude that a gate opening is not a plausible explanation of the observed isotherm shape. It can thus be due to a moderate affinity between the adsorbate molecules and pore walls.

To estimate the strength of the interaction between the studied adsorbates and the surface of **1**, we fitted the adsorption isotherms with the Dubinin–Astakhov (DA) equation, which is well adapted for the description of the adsorption in microporous sorbents:⁴⁵

$$W = W_0 \exp[-(A/E)^n]$$

where $A = RT \ln(P_s/P)$ (R , gas constant; T , temperature; P , pressure; P_s , saturation pressure at 298 K), E is the characteristic interaction energy (kJ/mol), W is the adsorbed amount, W_0 is the maximum amount adsorbed in the micropores, and n is the heterogeneity parameter ($1 < n < 5$). Figure 4 shows that the DA equation gives a fair description of the S-type shape of all isotherms. The characteristic energies are equal to 6 kJ/mol for H_2O and 7.6 kJ/mol for CH_3OH . A higher value obtained for CH_3OH is in line with a larger pore volume probed by this molecule. An even larger value of E obtained for CO_2 (10.5 kJ/mol) can be due to a high quadrupole moment of this molecule.

The value of the characteristic energy for H_2O allows one to assess the hydrophilicity of a microporous sorbent.⁴⁶ From this criterion, our material is closer to a hydrophilic NaY zeolite (10 kJ/mol) than to a hydrophobic activated carbon (1.3 kJ/mol).⁴⁶ More specifically, the hydrophilicity of **1** can be compared to that of other PCPs. This can be done using the value of P/P_s at which the solid adsorbs 50% of its maximum loading.⁴⁷ The corresponding value for **1** ($P/P_s = 0.1$; see Figure 4) is similar to the values observed for PCPs containing $-\text{NH}_2$ groups and

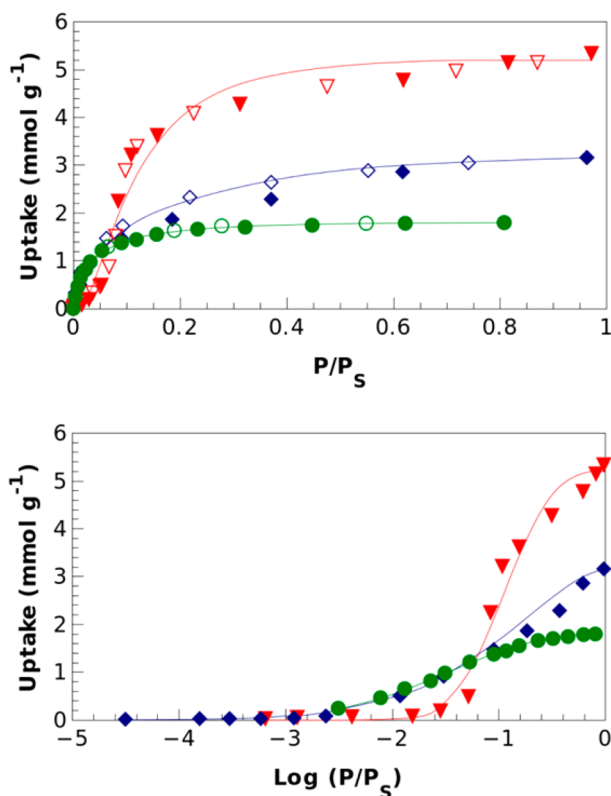


Figure 4. Adsorption isotherms of CH_3OH (blue), H_2O (red), and CO_2 (green) on **1** at 298 K on linear (top) and logarithmic (bottom) scales: full symbols, adsorption; empty symbols, desorption. The connecting lines correspond to the fit with the DA equation (see the text for details).

considered to be hydrophilic. PCPs have been considered as promising materials for H₂O adsorption for different applications such as heat exchangers or the delivery of H₂O in normal conditions,^{48–53} because they can fulfill the expected criteria for such a purpose: an easy release of H₂O, a high H₂O uptake capacity, a good cycling performance, etc. The PCP materials based on bipyridinium carboxylate linkers can be of interest in this field.

3.3. Adsorption of NH₃. The adsorption and desorption isotherms of NH₃ on **1** at 298 K reveal a high capacity of the solid toward NH₃ (Figure 5). The maximum adsorbed amount

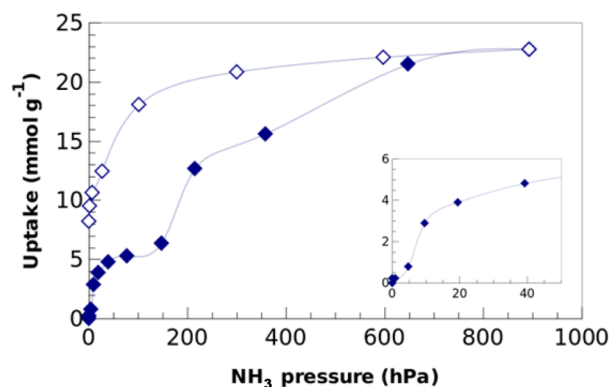


Figure 5. Adsorption and desorption of NH₃ on **1** at 298 K: full symbols, adsorption; empty symbols, desorption. Inset: low-pressure range. The connecting lines are guides for the eye.

of 22.8 mmol/g at 900 h-Pa [corresponding to 0.39 g(NH₃)/g] is one of the highest values reported to date. The isotherm has a rather complex shape and can be divided into two distinct regions.

In the low-pressure range (<150 h-Pa; see the inset), the shape of the isotherm is similar to that of H₂O (see Figure 4). We have also found that, if the adsorption is stopped below 150 h-Pa, the adsorbed NH₃ can be completely desorbed under vacuum at 298 K, and the crystalline structure of the sample after such an adsorption–desorption cycle is preserved. This observation shows that this part of the isotherm is fully reversible, and below 150 h-Pa, the pore filling occurs via the physisorption of NH₃ molecules.

At pressure higher than 150 h-Pa, the adsorbed amount strongly increases up to 22.3 mmol/g at 900 h-Pa due to chemisorption of NH₃ in **1**. This is evidenced by a pronounced hysteresis accompanied by retention of ca. 8.2 mmol(NH₃)/g even after the sample is maintained under a secondary vacuum for 48 h at 298 K (Figure 5). A complete desorption of NH₃ is only possible after heating for 1 h at 473 K (see below). The conclusion about the chemisorption is also confirmed by the loss of crystallinity in the solid after NH₃ adsorption ($P > 150$ h-Pa) and desorption at either 298 or 473 K (no diffraction lines in the PXRD patterns). Decomposition of the crystalline structure of **1** allows one to suppose that the interaction with NH₃ molecules at pressure higher than 150 h-Pa occurs mainly through their coordination to cadmium cations, which are known to be hexacoordinated in NH₃ complexes.⁵⁴ This ability of cadmium allows one to explain a high capacity of **1**: coordination of each cadmium by six NH₃ molecules would yield the loading of 14.25 mmol of NH₃ per g of **1**.

The evolution of the coordination sphere of cadmium upon adsorption and desorption of NH₃ was studied by ¹¹³Cd NMR

(Figure 6). Such a study is quite rare in this field.⁵⁵ The spectrum of the crystalline pristine sample (red line) shows

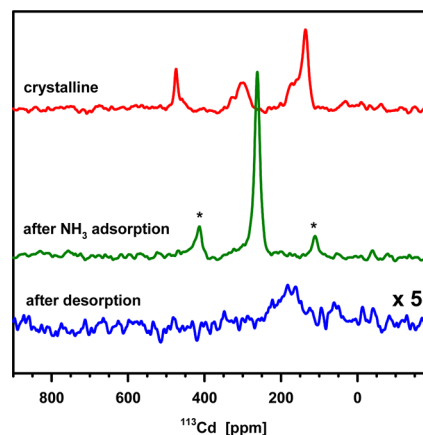


Figure 6. Solid-state ¹H–¹¹³Cd CP NMR spectra of the pristine sample of **1** (red) and the sample containing 8.2 mmol/g of NH₃ (green) and a direct excitation ¹¹³Cd NMR spectrum of **1** saturated with NH₃ and then regenerated at 473 K (blue). Asterisks denote spinning side bands.

three peaks corresponding to cadmium atoms occupying different crystallographic positions. We tentatively assign the sharp downfield signal at 475 ppm to Cd(2) with Cd(2)Cl₂O₄ coordination, the broad signal at 302 ppm to the disordered Cd(3)Cl₄^{2–}, and the upfield signal at 133–176 ppm to Cd(1)Cl₆ octahedra (for comparison, nonhydrated CdCl₂ was found at 183 ppm⁵⁶). The latter signal also shows a certain disorder. Note that CP spectra are not quantitative, and the signal intensity depends on the vicinity of the hydrogen atom if the molecular mobility is similar. The solid containing 8.2 mmol/g of NH₃, which was obtained after desorption at 298 K, yields, in contrast to the pristine sample, only one very intense peak whose position (262 ppm) is different from those of all three previous signals (green line). The local environment of the cadmium ions has changed, and despite the transformation to an amorphous phase, it has become more homogeneous. Furthermore, hydrogen atoms must be relatively close because the CP transfer is efficient. The chemical shift is close to those of Cd(NH₃)₆Cl₂ in 50:50 NH₃/D₂O, which have been determined as 274 and 287 ppm depending on the concentration.⁵⁷ (Note that in ref 57 the sense of the chemical shift is inverted.) These findings support the hypothesis that NH₃ molecules are coordinated to cadmium cations. A complete elimination of NH₃ after heating at 473 K results in a shift back toward a mixed oxygen–halogen cadmium environment, as evidenced by a strong broadening of the NMR signal, which reflects an extremely inhomogeneous environment of the cadmium ion (blue line). For this sample, CP transfer from hydrogen did not prove successful, potentially because of the longer distances of cadmium to hydrogen. In contrast, the ¹³C NMR spectrum does not change very much upon desorption (not shown). This difference in the sensitivity to the presence of NH₃ is another indication that the cadmium ions play a central role in the absorption of NH₃.

The conclusions based on the results of ¹¹³Cd NMR are confirmed by Fourier transform infrared (FTIR) spectroscopy. The spectrum of the sample containing 8.2 mmol/g of NH₃ shows the presence of its characteristic bands (Figure S5), but in addition, some bands in the range 1300–1700 cm^{–1} are

shifted (Figure S6). Comparison with the spectra of other MOFs^{58,59} allowed us to identify them as symmetric (ν_s) and asymmetric (ν_{as}) stretching modes of carboxylates. The splitting between these bands increases from 154 cm^{-1} in pristine **1** to 181 cm^{-1} in the sample containing 8.2 mmol/g of NH_3 (Figure S6). This increase is indicative of the transformation of bidentate carboxylates into ionic ones.⁶⁰ This finding confirms therefore our conclusion about the appearance of NH_3 in the coordination of cadmium atoms, which transforms the carboxylates from bidentate (see the structure of **1**) into “free” ionic groups. Upon NH_3 elimination, the carboxylates become again coordinated to cadmium, as follows from the close similarity between the spectrum of **1** and those of the regenerated samples (Figure S6).

In addition to coordination by Cd^{2+} cations, NH_3 molecules can be involved in redox reactions with bipyridinium-based ligands.³ The existence of such a reaction is confirmed by electron transfer from NH_3 to pc1 resulting in the formation of bipyridinium radicals. This process is suggested by the color change of **1** from brown to black (see the UV–vis spectra in Figure S4). Direct evidence of the formation of the bipyridinium radicals was provided by EPR spectroscopy (Figure 7). The spectrum of the as-synthesized sample contains

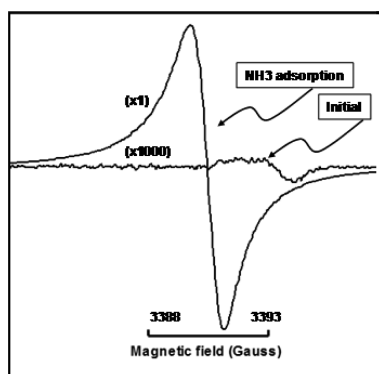


Figure 7. EPR spectra of pristine **1** and of a sample containing 8.2 mmol/g of NH_3 .

only a low-intensity signal originating from the EPR cavity. In contrast, after NH_3 adsorption [the sample containing 8.2 mmol(NH_3)/g], a clear signal is observed, revealing a quite high unpaired spin concentration (Figure 7). With such a concentration, the occurrence of exchange interactions explains the quasi-isotropic signal with $g = 2.0035$ and an EPR narrow line width of about 1.5 G. Moreover, the absence of hyperfine coupling between the unpaired spins and nitrogen nuclei from the bipyridinium units or with chlorine nuclei (superhyperfine coupling) is probably caused by the mobility of the unpaired electrons in the host structure. Electron transfer from NH_3 to bipyridinium moieties could produce some species containing nitrogen atoms with lower oxidation degree than in NH_3 .

Given the NMR and FTIR data, we can interpret the desorption behavior of the sample after full saturation in the following way. The sample saturated at 900 hPa of NH_3 (22.3 mmol/g) contains three types of NH_3 molecules: (i) physisorbed (~ 5 mmol/g); (ii) coordinated to cadmium (14.25 mmol/g for six NH_3 per cadmium); (iii) interacting with bipyridinium units (remaining 3.05 mmol/g). Upon decreasing NH_3 pressure, the physisorbed molecules are eliminated because of the reversibility of this interaction (see

above). At low NH_3 pressure, $\text{Cd}(\text{NH}_3)_6^{2+}$ can also partially decompose because the stoichiometric complex is known to be stable only in the presence of gaseous NH_3 .^{61,62} The NH_3 molecules retained in the solid after 48 h of evacuation (8.2 mmol/g) are therefore coordinated to cadmium (3–4 per cadmium) and/or interacting with the bipyridinium units. These strongly bound molecules can be fully eliminated only upon heating up to 473 K (Figure S7).

Reusability is an important characteristic of an adsorbent. Therefore, the sample (**1**) was tested during three successive cycles comprising NH_3 adsorption at 298 K and regeneration under vacuum at 473 K (Figure 8). Surprisingly, despite the

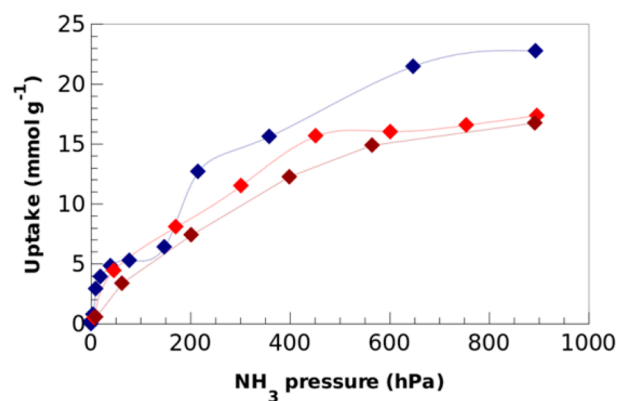


Figure 8. Three successive adsorption isotherms of NH_3 on **1** at 298 K: blue, first; red, second; brown, third. After each adsorption, the sample was regenerated at 473 K under vacuum. The connecting lines are guides for the eye.

amorphous nature of the solid obtained after the first cycle, we found that it is still able to adsorb an important volume of NH_3 (Figure 8). Indeed, the maximal adsorbed amount at 900 hPa is still 17.6 mmol/g after the first adsorption–regeneration cycle. Moreover, this value remains almost constant during the next cycle. The observed drop of the capacity between the first and second adsorption cycles of 5.2 mmol/g [from 22.8 to 17.6 mmol(NH_3)/g] is close to the amount adsorbed in the pores of pristine **1** (~ 5 mmol/g; inset in Figure 5). This fact suggests that the decrease of the capacity observed after the first adsorption is mostly due to the disappearance of pores provoked by the structure collapse. It is worth noting that the maximum adsorbed amount in the second cycle exceeds the number of NH_3 molecules that can be coordinated by cadmium (14.25 mmol/g). These additional molecules probably interact with the positively charged bipyridinium-based ligands. Also, one cannot exclude the existence of small irregular pores in the amorphous solid that are able to accommodate NH_3 molecules.

4. CONCLUSIONS

In this work, the synthesis, crystal structure, and adsorption properties of a novel PCP based on the zwitterionic bipyridinium carboxylate ligand pc1 are described. In the structure of **1**, hexagonal channels run along the c axis. We have first shown that H_2O or CH_3OH can be reversibly adsorbed, filling the channels with maximum uptake values at 298 K of 5.33 and 3.16 mmol/g, respectively. The observed shape of the adsorption isotherms is shown to be due to a moderate interaction strength between the guest molecules and walls of the channels. In contrast, **1** exhibits high NH_3 uptake among the best in the field of PCPs. A value of 22.3 mmol/g is reached

at $P = 900$ h·Pa after the first adsorption cycle. NH_3 molecules are first physisorbed in channels at low pressure (<150 h·Pa) and then chemisorbed at higher pressure. The chemisorption process involves, on the one hand, Cd^{2+} centers, as highlighted by solid-state ^{113}Cd NMR, and, on the other hand, the bipyridinium units. Although the sample becomes amorphous after the first adsorption cycle, the repeatability of the adsorption–desorption process has been proven, with an average NH_3 uptake of ca. 17 mmol/g.

■ ASSOCIATED CONTENT

Supporting Information

The Supporting Information is available free of charge on the ACS Publications website at DOI: 10.1021/acs.inorgchem.6b01119.

Synthesis procedures, summary of the X-ray crystal data, PXRD patterns of **1** and dehydrated **1**, TGA, UV–vis and FTIR spectra, and desorption curve of NH_3 under heating in a vacuum (PDF)
CIF file (CIF)

■ AUTHOR INFORMATION

Corresponding Authors

*E-mail: nicolas.mercier@univ-angers.fr.

*E-mail: igor.bezverkhyy@u-bourgogne.fr.

Author Contributions

The manuscript was written through contributions of all authors. All authors have given approval to the final version of the manuscript.

Notes

The authors declare no competing financial interest.

■ ACKNOWLEDGMENTS

M.L. thanks the University of Angers for a Ph.D. grant.

■ REFERENCES

- (1) Higuchi, M.; Tanaka, D.; Horike, S.; Sakamoto, H.; Nakamura, K.; Takashima, Y.; Hijikata, Y.; Yanai, N.; Kim, J.; Kato, K.; Kubota, Y.; Takata, M.; Kitagawa, S. *J. Am. Chem. Soc.* **2009**, *131*, 10336–10337.
- (2) Kano, P.; Matsuda, R.; Sato, H.; Li, L.; Jeon, H. J.; Kitagawa, S. *Inorg. Chem.* **2013**, *52*, 10735–10737.
- (3) Tan, B.; Chen, C.; Cai, L.-X.; Zhang, Y.-J.; Huang, X.-Y.; Zhang, J. *Inorg. Chem.* **2015**, *54*, 3456–3461.
- (4) Yao, Q.-X.; Pan, L.; Jin, X.-H.; Li, J.; Ju, Z.-F.; Zhang, J. *Chem. - Eur. J.* **2009**, *15*, 11890–11897.
- (5) Lin, J.-B.; Shimizu, G. K. H. *Inorg. Chem. Front.* **2014**, *1*, 302–305.
- (6) Toma, O.; Mercier, N.; Allain, M.; Kassiba, A. A.; Bellat, J.-P.; Weber, G.; Bezverkhyy, I. *Inorg. Chem.* **2015**, *54*, 8923–8930.
- (7) Aulakh, D.; Varghese, J. R.; Wriedt, M. *Inorg. Chem.* **2015**, *54*, 1756–1764.
- (8) Liu, J.-J.; Guan, Y.-F.; Lin, M.-J.; Huang, C.-C.; Dai, W.-X. *Cryst. Growth Des.* **2015**, *15*, 5040–5046.
- (9) Yao, Q. X.; Ju, Z. F.; Jin, X. H.; Zhang, J. *Inorg. Chem.* **2009**, *48*, 1266–1268.
- (10) Sun, J.-K.; Wang, P.; Chen, C.; Zhou, X.-J.; Wu, L.-M.; Zhang, Y.-F.; Zhang, J. *Dalton Trans.* **2012**, *41*, 13441–13446.
- (11) Sun, J.-K.; Wang, P.; Yao, Q.-X.; Chen, Y.-J.; Li, Z.-H.; Zhang, Y.-F.; Wu, L.-M.; Zhang, J. *J. Mater. Chem.* **2012**, *22*, 12212–12219.
- (12) Sun, J.-K.; Jin, X.-H.; Cai, L.-X.; Zhang, J. *J. Mater. Chem.* **2011**, *21*, 17667–17672.
- (13) Jin, X.-H.; Sun, J.-K.; Xu, X.-M.; Li, Z.-H.; Zhang, J. *Chem. Commun.* **2010**, *46*, 4695–4697.
- (14) Li, H.-Y.; Wei, Y.-L.; Dong, X.-Y.; Zang, S.-Q.; Mak, T. C. *Chem. Mater.* **2015**, *27*, 1327–1331.

- (15) Wang, M.-S.; Xu, G.; Zhang, Z.-J.; Guo, G.-C. *Chem. Commun.* **2010**, *46*, 361–376.
- (16) Mercier, N. *Eur. J. Inorg. Chem.* **2013**, *2013*, 19–31.
- (17) Leblanc, N.; Bi, W.; Mercier, N.; Auban-Senzier, P.; Pasquier, C. *Inorg. Chem.* **2010**, *49*, 5824.
- (18) Leblanc, N.; Allain, M.; Mercier, N.; Sanguinet, L. *Cryst. Growth Des.* **2011**, *11*, 2064–2069.
- (19) Monk, P. M. S. *The Viologens: Physicochemical Properties, Synthesis, and Application of the Salt of 4,4'-Bipyridine*; Wiley: New York, 1998.
- (20) Britt, D.; Tranchemontagne, D.; Yaghi, O. M. *Proc. Natl. Acad. Sci. U. S. A.* **2008**, *105*, 11623–11627.
- (21) Morris, W.; Doonan, C. J.; Yaghi, O. M. *Inorg. Chem.* **2011**, *50*, 6853–6855.
- (22) Spanopoulos, I.; Xydias, P.; Malliakas, C. D.; Trikalitis, P. N. *Inorg. Chem.* **2013**, *52*, 855–862.
- (23) Katz, M. J.; Howarth, A. J.; Moghadam, P. Z.; DeCoste, J. B.; Snurr, R. Q.; Hupp, J. T.; Farha, O. K. *Dalton Trans.* **2016**, *45*, 4150–4153.
- (24) Kajiwara, T.; Higuchi, M.; Yuasa, A.; Higashimura, H.; Kitagawa, S. *Chem. Commun.* **2013**, *49*, 10459–10461.
- (25) Petit, C.; Huang, L.; Jagiello, J.; Kenvin, J.; Gubbins, K. E.; Bandosz, T. J. *Langmuir* **2011**, *27*, 13043–13051.
- (26) Peterson, G. W.; Wagner, G. W.; Balboa, A.; Mahle, J.; Sewell, T.; Karwacki, C. J. *J. Phys. Chem. C* **2009**, *113*, 13906–13917.
- (27) Saha, D.; Deng, S. J. *Colloid Interface Sci.* **2010**, *348*, 615–620.
- (28) Kajiwara, T.; Higuchi, M.; Watanabe, D.; Higashimura, H.; Yamada, T.; Kitagawa, H. *Chem. - Eur. J.* **2014**, *20*, 15611–15617.
- (29) Petit, C.; Karwacki, C.; Peterson, G.; Bandosz, T. J. *J. Phys. Chem. C* **2007**, *111*, 12705–12714.
- (30) Petit, C.; Bandosz, T. J. *J. Phys. Chem. C* **2007**, *111*, 16445–16452.
- (31) Van Humbeck, J. F.; McDonald, T. M.; Jing, X.; Wiers, B. M.; Zhu, G.; Long, J. R. *J. Am. Chem. Soc.* **2014**, *136*, 2432–2440.
- (32) Doonan, C. J.; Tranchemontagne, D. J.; Glover, T. G.; Hunt, J. R.; Yaghi, O. M. *Nat. Chem.* **2010**, *2*, 235–237.
- (33) Das, R. R.; Lee, J.-M.; Noh, C.-H.; Jeon, S.-J. U.S. Patent Appl. Publ. 20120176658 A1 20120712, 2012.
- (34) Banerjee, S.; Ghosh, A.; Wu, B.; Lassahn, P.-G.; Janiak, C. *Polyhedron* **2005**, *24*, 593–599.
- (35) Banerjee, S.; Lassahn, P.-G.; Janiak, C.; Ghosh, A. *Polyhedron* **2005**, *24*, 2963–2971.
- (36) Mondal, S. S.; Bhunia, A.; Kelling, A.; Schilde, U.; Janiak, C.; Holdt, H.-J. *Chem. Commun.* **2014**, *50*, 5441–5443.
- (37) Mondal, S. S.; Bhunia, A.; Kelling, A.; Schilde, U.; Janiak, C.; Holdt, H.-J. *J. Am. Chem. Soc.* **2014**, *136*, 44–47.
- (38) Mondal, S. S.; Dey, S.; Baburin, I. A.; Kelling, A.; Schilde, U.; Seifert, G.; Janiak, C.; Holdt, H.-J. *CrystEngComm* **2013**, *15*, 9394–9399.
- (39) Mondal, S. S.; Bhunia, A.; Baburin, I. A.; Jäger, C.; Kelling, A.; Schilde, U.; Janiak, C.; Holdt, H.-J. *Chem. Commun.* **2013**, *49*, 7567–7570.
- (40) Bhunia, A.; Boldog, I.; Möller, A.; Janiak, C. *J. Mater. Chem. A* **2013**, *1*, 14990–14999.
- (41) Zhao, T.; Cuignet, L.; Dirtu, M. M.; Wolff, M.; Spasojevic, V.; Boldog, I.; Rotaru, A.; Garcia, Y.; Janiak, C. *J. Mater. Chem. C* **2015**, *3*, 7802–7812.
- (42) Cazorla-Amoros, D.; Alcaniz-Monge, J.; Linares-Solano, A. *Langmuir* **1996**, *12*, 2820–2824.
- (43) Rouquerol, F.; Rouquerol, J.; Sing, K. S. W.; Llewellyn, P.; Maurin, G. *Adsorption by Powders and Porous Solids*; Academic Press: Oxford, U.K., 2014.
- (44) Le Bail, A.; Duroy, H.; Fourquet, J. L. *Mater. Res. Bull.* **1988**, *23*, 447–452.
- (45) Dubinin, M. M. *Carbon* **1989**, *27*, 457–467.
- (46) Pires, J.; Pinto, M. L.; Carvalho, A.; de Carvalho, M. B. *Adsorption* **2003**, *9*, 303–309.
- (47) Canivet, J.; Fateeva, A.; Guo, Y.; Coasne, B.; Farrusseng, D. *Chem. Soc. Rev.* **2014**, *43*, 5594–5617.

- (48) Henninger, S. K.; Habib, H. A.; Janiak, C. *J. Am. Chem. Soc.* **2009**, *131*, 2776–2777.
- (49) Jeremias, F.; Khutia, A.; Henninger, S. K.; Janiak, C. *J. Mater. Chem.* **2012**, *22*, 10148–10151.
- (50) Khutia, A.; Rammelberg, H. U.; Schmidt, T.; Henninger, S.; Janiak, C. *Chem. Mater.* **2013**, *25*, 790–798.
- (51) Jeremias, F.; Lozan, V.; Henninger, S. K.; Janiak, C. *Dalton Trans.* **2013**, *42*, 15967–15973.
- (52) Jeremias, F.; Fröhlich, D.; Janiak, C.; Henninger, S. K. *RSC Adv.* **2014**, *4*, 24073–24082.
- (53) Fröhlich, D.; Henninger, S. K.; Janiak, C. *Dalton Trans.* **2014**, *43*, 15300–15304.
- (54) Nilsson, K. B.; Eriksson, L.; Kessler, V. G.; Persson, I. *J. Mol. Liq.* **2007**, *131–132*, 113–120.
- (55) Haldar, R.; Inukai, M.; Horike, S.; Uemura, K.; Kitagawa, S.; Maji, T. K. *Inorg. Chem.* **2016**, *55*, 4166–4172.
- (56) Sakida, S.; Shojiya, M.; Kawamoto, Y. *Solid State Commun.* **2000**, *115*, 553–558.
- (57) Cardin, A. D.; Ellis, P. D.; Odom, J. D.; Howard, J. W., Jr. *J. Am. Chem. Soc.* **1975**, *97*, 1672–1679.
- (58) Bernini, M. C.; Garro, J. C.; Brusau, E. V.; Narda, G. E.; Varetti, E. L. *J. Mol. Struct.* **2008**, *888*, 113–123.
- (59) Bernini, M. C.; Gandara, F.; Iglesias, M.; Snejko, N.; Gutiérrez-Puebla, E.; Brusau, E. V.; Narda, G. E.; Monge, M. A. *Chem. - Eur. J.* **2009**, *15*, 4896–4905.
- (60) Deacon, G. B.; Phillips, R. J. *Coord. Chem. Rev.* **1980**, *33*, 227–250.
- (61) Jenkins, T. E.; Ferris, L. T. H.; Bates, A. R.; Gillard, R. D. J. *Phys. C: Solid State Phys.* **1977**, *10*, L521–L526.
- (62) Migdal-Mikuli, A.; Mikuli, E.; Zabinska, K. *J. Phys. C: Solid State Phys.* **1982**, *15*, 6565–6571.